Dalton Transactions

This article can be cited before page numbers have been issued, to do this please use: S. She, Y. Li and W. Li, *Dalton Trans.*, 2016, DOI: 10.1039/C6DT00951D.

ROYAL SOCIETY OF CHEMISTRY

www.rsc.org/dalton

View Article Online
DOI: 10.1039/C6DT00951D

Journal Name

RSCPublishing

ARTICLE

Cite this: DOI: 10.1039/x0xx00000x

Received 00th January 2012,
Accepted 00th January 2012

DOI: 10.1039/x0xx00000x

www.rsc.org/

Two 3d-4f double helical chains including $[Dy_2M_2]_n$ (M = Ni^{II} and Co^{II}) cores exhibiting slow magnetic relaxation

Shixiong She,[a] Yahong Li*[a] and Wu Li[b]

Two new 3d-4f heterometallic 1D chains of formulas $\{[Dy_2M_2L_4(NO_3)(H_2O)_3][Dy_2M_2L_4(NO_3)(CH_3COO)(H_2O)_2]\cdot NO_3\cdot 12H_2O\cdot 2C_2H_5OH\}_n$ [M = Ni (**1**); Co (**2**)] have been prepared using the multidentate ligand 2-{[(2-hydroxy-3-methoxyphenyl)methylidene]amino}benzoic acid (H_2L), which has NO and OO' chelating pockets that are able to selectively encapsulate Ln^{III} and transition metal ions, respectively. Crystal structure analyses reveal that two complexes are isostructural and display one-dimensional ladder-like double helical chain structures, in which the two single helical chains $\{[Dy_2M_2L_4(NO_3)(H_2O)_3]^+\}$ and $\{Dy_2M_2L_4(NO_3)(CH_3COO)(H_2O)_2\}$ (M = Ni(**1**), Co(**2**)) both run along *c*-axis and have opposite chirality. Complexes **1** and **2** represent the first example of 3d-4f double-chain frameworks in which the compositions of the two individual chains are different. Variable temperature dc magnetic susceptibility studies reveal different strength of ferromagnetic interactions between magnetic centers in **1** and **2**, which is mainly attributed to the different metal centers and finally result in the distinctive magnetic dynamic behaviors.

Introduction

Molecular magnetic materials, including single molecule magnets (SMMs) and single-chain magnets (SCMs), have received enormous attention over the past decades due to their potential applications in quantum computations, high-density data storage and molecular spintronics.[1,2] During early researches on SMMs, a large number of complexes based on 3d metal ions were synthesized in order to achieve large effective barrier (U_{eff}).[3] Despite of extremely large spin values, some complexes did not behave as SMMs due to the lack of Ising-type magnetic anisotropy, suggesting that single ion anisotropy is the crucial factor for designing SMMs.[4] After the first discovery of lanthanide-SMM (4f-SMM) in 2003 with an energy barrier of U_{eff} = 230 K,[5] a plethora of pure 4f-SMMs have been obtained,[6] due to the large total angular moment (J) and single-ion anisotropy of 4f metal ions.[7] However, there are two major obstacles to construct 4f-SMMs with superior magnetic properties, including the quantum tunneling that lowers the effective relaxation energy barrier and very weak interactions between Ln^{3+} ions which result in lower spin ground state than that for a single ion.[8]

It has been reported that the merge of 3d metal ions with 4f spin carriers would be a promising strategy to assemble SMMs, since the intermediate magnetic exchange between 3d and 4f ions may effectively reduce quantum tunneling of the magnetization (QTM) and result in longer relaxation times.[9]

Up to now, many 3d-4f heterometallic complexes have been synthesized. In these complexes, 3d ions such as Co^{II}, Ni^{II}, Mn^{III} and Fe^{III} have been chosen due to their stronger magnetic anisotropy;[10] Tb^{III} and Dy^{III} ions have commonly been employed because they possess intrinsic high-spin and strong Ising-type anisotropy, therefore fulfilling the requirements of slow relaxation of the magnetization.[11] However, due to the specific chemical natures of 3d and 4f ions, the synthetic approaches that could rationally integrate 3d and 4f ions into one system are still less developed. The synthetic challenge involves discovering a suitable ligand which could incorporate different metal ions into a single molecular entity or a 1D chain system, giving heterometallic complexes with interesting topologies and magnetic properties. Different kinds of organic ligands, *e.g.*, oximes,[12] amino acids,[13] aminopolyalcohols,[14] Schiff bases,[9] *etc.*, have been used to produce new types of 3d-4f compounds.

In the present work, we have used 2-{[(2-hydroxy-3-methoxyphenyl)methylidene]amino}benzoic acid (H_2L)[15] for the synthesis of Dy^{III}-Ni^{II} and Dy^{III}-Co^{II} 1D chain complexes. By introducing carboxyl and hydroxyl groups into the ligand, H_2L has NO and OO' coordination pockets with preference for transition metal ions and Ln^{III} ions. Meanwhile, it has been shown that the exchange interaction between Dy^{III} and Ni^{II} in Dy^{III}-Ni^{II} compounds is ferromagnetic.[16] Two new heterometallic complexes of formulas $\{[Dy_2M_2L_4(NO_3)(H_2O)_3][Dy_2M_2L_4(NO_3)(CH_3COO)(H_2O)_2]\cdot NO_3\cdot 12H_2O\cdot 2C_2H_5OH\}_n$ [M = Ni (**1**); Co (**2**)] were isolated by the reactions of H_2L, $Dy(NO_3)_3\,6H_2O$, and $Ni(CH_3COO)_2\,4H_2O$ (or $Co(CH_3COO)_2\,4H_2O$) under the solvothermal conditions. Their syntheses, structures, and magnetic properties are described in detail in this paper.

View Article Online
DOI: 10.1039/C6DT00951D

Experimental section

All solvents and reagents were obtained from commercial sources and used as received without further purification. The Schiff base ligand (H_2L) was prepared by a condensation reaction between o-vanillin and 2-aminobenzoic acid in 1:1 molar ratio in methanol.[15]

Syntheses of complexes

$\{[Dy_2Ni_2L_4(NO_3)(H_2O)_3][Dy_2Ni_2L_4(NO_3)(CH_3COO)(H_2O)_2]\cdot NO_3\cdot 12H_2O\cdot 2C_2H_5OH\}_n$ (1). A mixture of $Dy(NO_3)_3\ 6H_2O$ (0.054 g, 0.12 mmol), $Ni(CH_3COO)_2\ 4H_2O$ (0.024 g, 0.12 mmol), H_2L (0.020 g, 0.075 mmol) was dissolved into ethanol (4 mL) and water (4 mL), and then this solution was sealed in a glass tube. The tube was heated at 75 ℃ for 2 days. After cooling to room temperature, red crystals of **1** were obtained in 35% yield based on Dy. Elemental analysis (%) calcd for $C_{126}H_{137}Ni_4Dy_4N_{11}O_{62}$: C, 41.10; H, 3.75; N, 4.18. Found C, 38.23; H, 3.75; N, 4.02. Selected IR data (KBr, cm^{-1}): 3404 s, 1620 s, 1597 s, 1544 s, 1470 s, 1384 s, 1298 m, 1235 s, 1195 s, 1095 s, 966 m, 853 w, 769 w, 741 m, 709 w, 642 w, 539 w.

$\{[Dy_2Co_2L_4(NO_3)(H_2O)_3][Dy_2Co_2L_4(NO_3)(CH_3COO)(H_2O)_2]\cdot NO_3\cdot 12H_2O\cdot 2C_2H_5OH\}_n$ (2). Complex **2** was obtained by the same procedure as that of **1**, using $Co(CH_3COO)_2\ 4H_2O$ in place of $Ni(CH_3COO)_2\ 4H_2O$. Yield of **2** is 41% based on Dy. Elemental analysis (%) calcd for $C_{126}H_{137}Co_4Dy_4N_{11}O_{62}$: C, 41.09; H, 3.75; N, 4.18. Found C, 38.01; H, 3.78; N, 3.96. Selected IR data (KBr, cm^{-1}): 3373 s, 2972 m, 1619 s, 1597 s, 1582 m, 1540 s, 1470 m, 1456 m, 1385 s, 1298 m, 1235 s, 1194 s, 1094 s, 1049 s, 969 m, 879 m, 767 w, 738 m, 710 w, 640 w, 537 w.

X-ray diffraction crystallography

Data were collected at room temperature on Bruker Smart ApexII diffractometer equipped with a graphite monochromator utilizing Mo Kα radiation; the ω-2θ scan technique was applied. The structures were solved by direct methods using SHELXS-97and refined on F^2 using full-matrix least-squares with SHELXL-97.[17] In addition to the refined lattice solvents the crystal structures contained significant pores (8430 and 7870 $Å^3$ for **1** and **2** respectively) containing the highly disordered solvents that could not be satisfactorily refined. The SQUEEZE routine of PLATON was used in the treatment of the crystallographic data. Some lattice solvents may have been rapidly lost once crystals were removed from the mother liquor, and SQUEEZE may not always give a completely accurate determination of residual electrons. Despite the difficulty in crystallographically determining the lattice solvents, the composition and connectivity of complexes **1** and **2** are unambiguous. The refinement details for the new complexes reported in this work are summarized in Table 1. See CIF files for further details.

Results and discussion

Descriptions of structures

The X-ray diffraction analysis indicates they both crystallize in the tetragonal system with the space group $I4_1$. As the two complexes are isostructural, complex **1** is chosen to depict the structure in detail. Complex **1** consists of two single-helical chains of formulas $\{[Dy_2Ni_2L_4(NO_3)(H_2O)_3]^+\}$ and $\{Dy_2Ni_2L_4(NO_3)(CH_3COO)(H_2O)_2\}$, one nitrate ion as counterion to compensate the charge of the $\{[Dy_2Ni_2L_4(NO_3)(H_2O)_3]^+\}$ chain, 12 solvent water molecules and 2 solvent ethanol molecules. The compositions of the two chains are different. As shown in Fig. 1, in the chain of $\{[Dy_2Ni_2L_4(NO_3)(H_2O)_3]^+\}$, the asymmetric unit consists of two Dy^{III} ions, two Ni^{II} ions, four L^{2-} ligands, one NO_3^- ion and three water molecules. The coordination environments of the two Ni^{II} ions are identical (Fig. S1). Each Ni^{II} ion possesses a slightly elongated octahedral geometry, in which the equatorial plane is formed by N_2O_2 atoms from two L^{2-} ligands and the two axial positions are occupied by two carboxylate oxygen atoms from the same L^{2-} ligands. The axial bond lengths (Ni-O 2.082-2.097 Å) are relatively longer than the equatorial ones (Ni-O/N 2.016-2.034 Å). The coordination environments of Dy1 and Dy2 ions in the chain of $\{[Dy_2Ni_2L_4(NO_3)(H_2O)_3]^+\}$ are different. The Dy1 center has the {DyO9} coordination environment which is comprised of two phenolate oxygen atoms, two methoxy oxygen atoms and one carboxylate oxygen atom from three L^{2-} ligands, two oxygen atoms from one chelating nitrate anion, and two oxygen atoms from two water molecules. The Dy2 center is eight coordinated with a $\{DyO_8\}$ environment, with two phenolate oxygen atoms, two methoxy oxygen atoms and one carboxylato oxygen atom being from three L^{2-} ligands, and three oxygen atoms being from three water molecules. It is worth to note that the neighboring Ni^{II} and Dy^{III} ions are bridged by two modes. In the first mode, the metal ions are doubly bridged by two phenolato oxygen (μ_2-O) atoms from two L^{2-} ligands to form a DyNiO2 rhombus with angles in the range of 104.12(19)-108.36(19)°, 66.29(15)-66.89(16)° and 78.09(17)-79.00(18)° for Dy-O-Ni, O-Dy-O and O-Ni-O, respectively. The distances are 3.5013(10) Å for Dy1-Ni1, and 3.4986(11) Å for Dy2-Ni2. In the other mode, two carboxylate ions belonging to two L^{2-} ligands and displaying a μ_2-η^1:η^1 bridging mode link two pairs of Dy^{III} and Ni^{II} ions. The distances are 5.8528(15) Å for Dy1-Ni2, and 6.1546(16) Å for Dy2-Ni1. Thus, the two Dy^{III} ions and two Ni^{II} ions are connected together to give a $[Dy_2Ni_2]$ unit. The adjacent $[Dy_2Ni_2]$ units are further connected by two carboxylate oxygen atoms of two L^{2-} ligands to generate a ladder-like single-helical chain along *c*-axis, with a pitch of 22.9224 Å based on the repeat unit of two $[Dy_2Ni_2]$ moieties and two connecting carboxylate groups.

View Article Online
DOI: 10.1039/C6DT00951D

Table 1 Crystal data and structure refinement for complexes **1** and **2**

	1	**2**
Empirical formula	$C_{126}H_{137}Dy_4Ni_4N_{11}O_{62}$	$C_{126}H_{137}Co_4Dy_4N_{11}O_{62}$
Formula weight	3682.27	3683.24
Temperature/*K*	291(2)	291(2)
Crystal system	tetragonal	tetragonal
Space group	$I4_1$	$I4_1$
a/Å	26.2770(12)	26.2860(12)
c/Å	44.4110(15)	44.3921(15)
Volume/Å^3	30665(3)	30673(3)
Z	8	8
ρ_{calc} g/cm^3	1.595	1.595
μ/mm^{-1}	2.495	2.436
F(000)	14736.0	14704.0
Crystal size/mm^3	0.290 × 0.150 × 0.130	0.240 × 0.220 × 0.200
Radiation	MoKα (λ = 0.71073)	MoKα (λ = 0.71073)
2*θ* range for data collection/ °	3.158 to 56.612	1.8 to 56.616
Index ranges	$-33 \le h \le 34$, $-26 \le k \le 34$, $-54 \le l \le 58$	$-35 \le h \le 31$, $-28 \le k \le 35$, $-59 \le l \le 59$
Reflections collected	111960	112866
Independent reflections	36977 [R_{int} = 0.0453, R_{sigma} = 0.0547]	37997 [R_{int} = 0.0273, R_{sigma} = 0.0558]
Data/restraints/parameters	36977/1/1713	37997/2131/1753
Goodness-of-fit on F^2	1.005	0.865
Final *R* indexes [I>=2σ (I)]	R_1 = 0.0336, wR_2 = 0.0688	R_1 = 0.0222, wR_2 = 0.0451
Final *R* indexes [all data]	R_1 = 0.0618, wR_2 = 0.0797	R_1 = 0.0348, wR_2 = 0.0467
Largest diff. peak/hole / e Å^{-3}	0.93/-0.75	0.51/-0.30
Flack parameter	0.533(6)	0.400(4)

In the chain of $\{Dy_2Ni_2L_4(NO_3)(CH_3COO)(H_2O)_2\}$, the asymmetric unit consists of two Dy^{III} ions, two Ni^{II} ions, four L^{2-} ligands, one NO_3^- ion, one acetate ion and two water molecules. The coordination spheres of two Ni^{II} ions are the same as those of Ni^{II} ions in the chain of $\{[Dy_2Ni_2L_4(NO_3)(H_2O)_3]^+\}$. The coordination environment of Dy3 in the chain of $\{Dy_2Ni_2L_4(NO_3)(CH_3COO)(H_2O)_2\}$ is the same as that of Dy1 in the chain of $\{[Dy_2Ni_2L_4(NO_3)(H_2O)_3]^+\}$, while the coordination environment of Dy4 is different from that of Dy2. The Dy4 centre is eight coordinated with a $\{DyO_8\}$ mode, with two phenolato oxygen atoms, two methoxy oxygen atoms and one carboxylato oxygen atom being from three L^{2-} ligands, two oxygen atoms being from water molecules and one oxygen atom being from the acetate ion. The Dy^{III} ions and Ni^{II} ions are alternatively connected by phenolato oxygen atoms and carboxylate groups to form a $[Dy_2Ni_2]$ unit. The adjacent two $[Dy_2Ni_2]$ units are linked by two carboxylate groups to generate a ladder-like single-helical chain along *c*-axis, with a pitch of 23.1184 Å, slightly longer than that of $\{[Dy_2Ni_2L_4(NO_3)(H_2O)_3]^+\}$ chain. The distances are 3.4978(10) Å for Dy3-Ni3, 3.5037(11) Å for Dy4-Ni4, 5.7617(15) Å for Dy3-Ni4 and 6.2197(16) Å for Dy4-Ni3, close to the corresponding values in the chain of $\{[Dy_2Ni_2L_4(NO_3)(H_2O)_3]^+\}$.

The most fascinating feature of complex **1** is that two single helical chains all run along *c*-axis with opposite chirality, displaying an unusual "DNA"-shaped motif with ladder-like double-chain structure (Fig. 2).

Complexes **1** and **2** are members of a small family of heterometallic compounds with double-chain frameworks.[18] However, complexes **1** and **2** are the first reported 3d-4f double-chain frameworks in which the compositions of the two individual chains are different, demonstrating the novelty of this work.

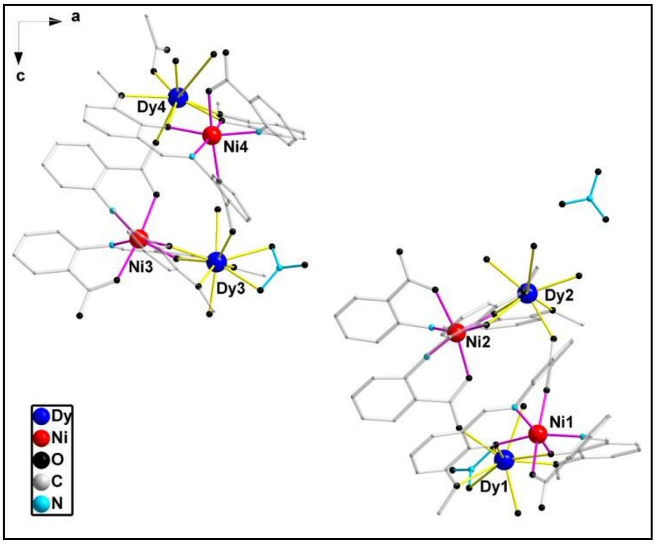

Fig. 1 Asymmetric units in the chains of $\{[Dy_2Ni_2L_4(NO_3)(H_2O)_3]^+\}$ and $\{Dy_2Ni_2L_4(NO_3)(CH_3COO)(H_2O)_2\}$ in compound **1**. Hydrogen atoms and crystallization solvent molecules have been omitted for clarity.

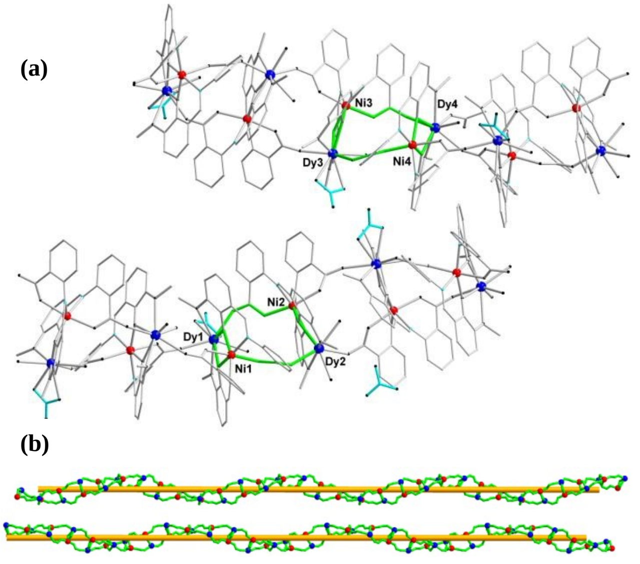

Fig. 2 (a) The structures of the chains of $\{[Dy_2Ni_2L_4(NO_3)(H_2O)_3]^+\}$ and $\{Dy_2Ni_2L_4(NO_3)(CH_3COO)(H_2O)_2\}$ in **1**. (b) The ladder-like shape and the arrangements of Dy^{III} and Ni^{II} ions in **1**.

Thermal studies of 1 and 2

Complexes **1** and **2** were studied by TG-DSC (Fig. S2, S3). It is noticed that the crystals of the two complexes quickly lose solvent molecules during the isolation process and turn opaque. As for **1**, the calculated mass loss corresponding to the solvent guests from the crystals and all water molecules bound to the metal centers

View Article Online
DOI: 10.1039/C6DT00951D

between 100 and 300 ℃ is 10.81%. However, the experimental result is 11.32%, this indicates that one water molecule (calc. 0.48%) from the mother liquor might be contained during the test process. The TG analysis of **2** shows a mass loss of 10.90% between 100 and 300 ℃, fully consistent with the calculated result (calc. 10.80%). However, it also shows a 9.08% mass loss around 51.5 ℃, which could be attributed to remaining solvents coming from the mother liquor.

Magnetic studies of 1 and 2

Variable-temperature magnetic measurements were performed with polycrystalline samples of **1** at an applied magnetic field of 1 kOe in the range of 2−300 K (Fig. 3). The $\chi_M T$ value of **1** at room temperature is 62.28 emu mol^{-1} K for two [Dy$_2$Ni$_2$] units, a value which is as expected for four magnetically isolated Dy^{III} ions and four magnetically noninteracting Ni^{II} ions (g = 4/3, J = 15/2 for Dy^{III} and g = 2, S = 1 for Ni^{II}). Upon cooling, the $\chi_M T$ value gradually increases to 63.21 emu mol^{-1} K at 140 K, which probably was ascribed to weak ferromagnetic interactions between the paramagnetic centers. Then $\chi_M T$ value further increases to a sharp peak value of 69.15 emu mol^{-1} K at 4 K before decreasing again to 67.78 emu mol^{-1} K at 2 K, indicating ferromagnetic coupling between paramagnetic centers.

The field dependence of the magnetization for complex **1** was collected at 2, 3, 4, 5 and 8 K (Fig. 4). The magnetization revealed nonsuperposition plots and similar rapid increase in the very low field region, which eventually reaches the value of 51.42 Nβ at 2 K and 7 T (Fig. S4), without saturation, suggesting the presence of magnetic anisotropy and/or considerable crystal-field effects.[19]

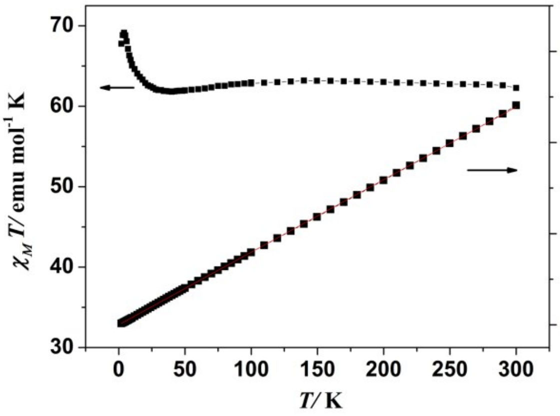

Fig. 3 Temperature dependence of magnetic susceptibilities in the form of $\chi_M T$ vs. T and χ_M^{-1} vs. T for **1** at 1 kOe. The solid line of the χ_M^{-1} vs. T illustration corresponds to the best fit from 300 K to 2 K.

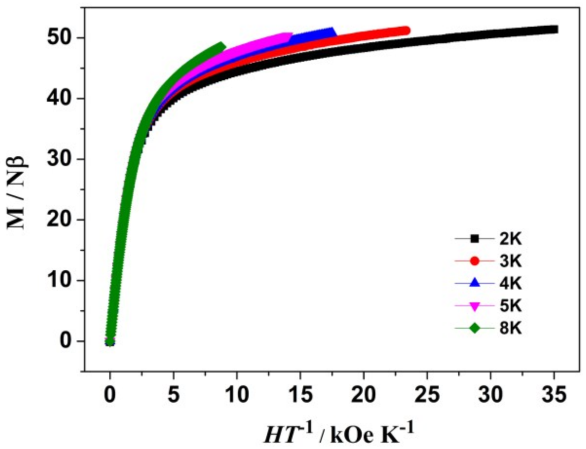

Fig. 4 M vs H/T plots at different temperatures below 8 K for **1.**

To further understand the magnetism of **1**, ac dynamic susceptibility measurements were performed in the temperature range 20-2 K at an oscillating 2.0 Oe field for variable frequencies (from 999 to 32 Hz). Both in- and out-of-phase signals show frequency dependence without peaks, suggesting a slow relaxation behavior of the magnetization. This is consistent with the hysteresis measurement in which no hysteresis displays at 2 K (Fig. 5, Fig. S5). Since the maxima in the plots of χ'' versus T can not be observed even up to 999 Hz, a dc field of 1 kOe were applied to the system in ac measurements. An increase in χ'' with still no peak shapes were obtained however, which can be attributed to the presence of a fast relaxation of the magnetization through a quantum tunneling mechanism.

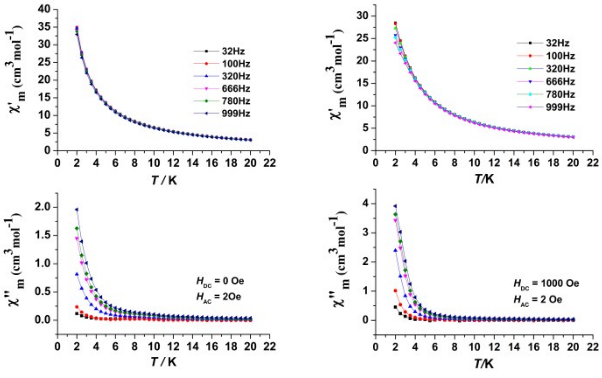

Fig. 5 Left: temperature dependence of the in-phase χ' and out-of-phase χ'' at different frequencies and a zero dc field for **1;** right: temperature dependence of the in-phase χ' and out-of-phase χ'' at different frequencies and a 1000 Oe dc field for **1**.

To investigate the influence of the metal ion on the magnetic properties, magnetic measurements on **2** were performed. The magnetic behaviors of **2** are different to those of **1** (Fig. 6). At 300 K, the $\chi_M T$ value is 73.73 emu mol^{-1} K for compound **2**, larger than the expected value for four magnetically noninteracting Co^{II} ions (S = 3/2, g = 2) and four magnetically isolated Dy^{III} ions (J = 15/2, g = 4/3). As reported in many other Co-containing compounds, the room temperature $\chi_M T$ value is usually higher than the expected spin-only one because of the orbital contribution of the high-spin Co^{II} ions.[14] Upon cooling from 300 to 2 K, the $\chi_M T$ values decrease gradually and then more rapidly below 170 K to the minimum value of 57.37 emu mol^{-1} K at 10 K, which may be resulted from Stark level splitting in the lanthanide ions in the weak crystal-field. After that $\chi_M T$ value appears a slight increase until 2 K and reaches 59.76 emu mol^{-1} K, indicating that very weak ferromagnetic coupling within the spin centers occurs.[20]

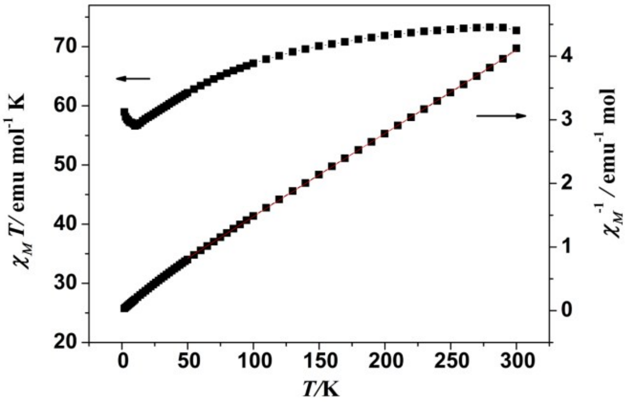

Fig. 6 Temperature dependence of magnetic susceptibilities in the form of $\chi_M T$ vs. T and χ_M^{-1} vs. T for **2** at 1 kOe. The solid line of the χ_M^{-1} vs. T illustration corresponds to the best fit from 300 K to 50 K

Dynamic studies of complex **2** have been explored under the same measurement conditions for complex **1**. As shown in Fig. S7, all of the signals of χ' and χ'' are very weak but frequency-dependent without any peaks occurring. Furthermore, the ac susceptibility was measured under 2000 Oe dc field at 999 Hz, no peaks neither in phase nor out of phase were found (Fig. S8). There are two factors may responsible for this phenomenon, namely, quantum tunneling and anti-ferromagnetic interactions.

As reported before, the magnetic property of Co^{II} system is usually in marked contrast with the Ni^{II} system with a similar structure.[21] It is usually considered that ferromagnetic interactions were in favor of SMMs behavior due to larger ground state. The differences in the strength of ferromagnetic interactions between magnetic centers in **1** and **2** may finally result in different magnetic properties of the two complexes.

Conclusions

In summary, two new 3d-4f heterotetrametallic 1D double-chain frameworks built from $[Dy_2M_2]_n$ (M = Ni(**1**), Co(**2**)) unit have been successfully obtained using 2-{[(2-hydroxy-3-methoxyphenyl)methylidene]amino}benzoic acid (H_2L) as the ligand under solvothermal conditions. They both exhibit ladder-like double-chain structures with two single-helical chains running along *c*-axis and possessing opposite chirality. Different magnetic dynamic behaviors were observed in **1** and **2**, which is may be associated with distinct magnetic interactions of different metal centers. The synthetic strategy used in this work will be further extended for obtaining more molecule-based magnetic materials with desired properties.

Acknowledgements

The authors appreciate the financial support from Natural Science Foundation of China (21272167), and A Project Funded by the Priority Academic Program Development of Jiangsu Higher Education Institution.

Notes and references

[a] *College of Chemistry, Chemical Engineering and Materials Science, Soochow University, Suzhou 215123, China. E-mail: liyahong@suda.edu.cn*
[b] *Qinghai Institute of Salt Lakes, Chinese Academy of Sciences, Xining 810008, China.*

CCDC 1030935 and 1030933 for complexes **1** and **2**, respectively.

References

1 (*a*) R. E. P. Winpenny, in *Comprehensive Coordination Chemistry II*, ed. J. A. McCleverty and T. J. Meyer, Elsevier, Amsterdam, 2004, vol. **7**, 125-175; (*b*) O. Kahn, *Magnetism: A Supramolecular Function* (NATO Science Series), 1995; (*c*) J. W. Steed and J. L. Atwood, *Supramolecular Chemistry* (Wiley), 2000; (*d*) D. Gatteschi, R. Sessoli and J. Villain, *Molecular Nanomagnets*, Oxford University Press, Oxford, 2006.

2 (*a*) M. N. Leuenberger and D. Loss, *Nature*, 2001, **410**, 789-793; (*b*) D. L. Long, E. Burkholder and L. Cronin, *Chem. Soc. Rev.*, 2007, **36**, 105-121; (*c*) A. R. Rocha, V. M. García-Suárez, S. W. Bailey, C. J. Lambert, J. Ferrerand and S. Sanvito, *Nat. Mater.*, 2005, **4**, 335-339; (*d*) A. J. Tasiopoulos, A. Vinslava, W. Wernsdorfer, K. A. Abboud and G. Christou, *Angew. Chem., Int. Ed.*, 2004, **43**, 2117-2121; (*e*) R. Vincent, S. Klyatskaya, M. Ruben, W. Wernsdorfer and F. Balestro, *Nature*, 2012, **488**, 357-360; (*f*) D. M. Low, L. F. Jones, A. Bell, E. K. Brechin, T. Mallah, E. Riviere, S. J. Teat and E. J. L. McInnes, *Angew. Chem., Int. Ed.*, 2003, **42**, 3781-3784; (*g*) M. Ganzhorn, S. Klyatskaya, M. Ruben and W. Wernsdorfer, *Nat. Nanotechnol.*, 2013, **8**, 165-169; (*h*) A. Candini, S. Klyatskaya, M. Ruben, W. Wernsdorfer and M. Affronte, *Nano Lett.*, 2011, **11**, 2634-2639; (*i*) R. Vincent, S. Klyatskaya, M. Ruben, W. Wernsdorfer and F. Balestro, *Nature*, 2012, **488**, 357-360; (*j*) S. T. Liddle and J. van Slageren, *Chem. Soc. Rev.*, 2015, **44**, 6655-6669; (*k*) Y. Z. Zheng, Z. P. Zheng and X. M. Chen, *Coord. Chem. Rev.*, 2014, **258-259**, 1-15; (*l*) H. L. Sun, Z. M. Wang and S. Gao, *Coord. Chem. Rev.*, 2010, **254**, 1081-1100.

3 (*a*) M. Soler, W. Wernsdorfer, K. Folting, M. Ping and G. Christou, *J. Am. Chem. Soc.*, 2004, **126**, 2156-2165; (*b*) A. J. Tasiopoulos, A. Vinslava, W. Wernsdorfer, K. A. Abboud and G. Christou, *Angew. Chem., Int. Ed.*, 2004, **43**, 2117-2121.

4 J. F. Wu, L. Zhao, P. Zhang, L. Zhang, M. Guo and J. K. Tang, *Dalton Trans.*, 2015, **44**, 11935-11942.

View Article Online
DOI: 10.1039/C6DT00951D

5 N. Ishikawa, M. Sugita, T. Ishikawa, S.-Y. Koshihara and Y. Kaizu, *J. Am. Chem. Soc.*, 2003, **125**, 8694-8695.

6 (*a*) L. Sorace, C. Benelli and D. Gatteschi, *Chem. Soc. Rev.*, 2011, **40**, 3092-3104; (*b*) Y. N. Guo, G. F. Xu, W. Wernsdorfer, L. Ungur, Y. Guo, J. K. Tang, H. J. Zhang, L. F. Chibotaru and A. K. Powell, *J. Am. Chem. Soc.*, 2011, **133**, 11948-11951; (*c*) H. Q. Tian, M. Wang, L. Zhao, Y. N. Guo, Y. Guo, J. K. Tang and Z. L. Liu, *Chem. Eur. J.*, 2012, **18**, 442-445.

7 V. Chandrasekhar, S. Hossain, S. Das, S. Biswas and J. P. Sutter, *Inorg. Chem.*, 2013, **52**, 6346-6353.

8 F. Tuna, C. A. Smith, M. Bodensteiner, L. Ungur, L. F. Chibotaru, E. J. L. McInnes, R. E. P. Winpenny, D. Collison and R. A. Layfield, *Angew. Chem., Int. Ed.*, 2012, **51**, 6976-6980.

9 K. Liu, W. Shi and P. Cheng, *Coord. Chem. Rev.*, 2015, **289-290**, 74-122.

10 (*a*) F. Pointillart, K. Bernot, R. Sessoli and D. Gatteschi, *Chem. Eur. J.*, 2007, **13**, 1602-1609; (*b*) C. Benelli and D. Gatteschi, *Chem. Rev.*, 2002, **102**, 2369-2387; (*c*) L. Sorace, C. Benelli and D. Gatteschi, *Chem. Soc. Rev.*, 2011, **40**, 3092-3104.

11 (*a*) S. D. Jiang, B. W. Wang, G. Su, Z. M. Wang and S. Gao, *Angew. Chem., Int. Ed.*, 2010, **49**, 7448-7451; (*b*) M. Jeletic, H. P. Lin, J. J. Le Roy, I. Korobkov, S. I. Gorelsky and M. Murugesu, *J. Am. Chem. Soc.*, 2011, **133**, 19286-19289; (*c*) F. Tuna, C. A. Smith, M. Bodensteiner, L. Ungur, L. F. Chibotaru, E. J. L. Mcinnes, R. E. P. Winpenny, D. Collison and R. A. Layfield, *Angew. Chem., Int. Ed.*, 2012, **51**, 6976-6980; (*d*) Y. N. Guo, G. F. Xu, W. Wernsdorfer, L. Ungur, Y. Guo, J. K. Tang, H. J. Zhang, L. F. Chibotaru and A. K. Powell, *J. Am. Chem. Soc.*, **2011**, *133*, 11948-11951.

12 C. J. Milios, A. Vinslava, W. Wernsdorfer, A. Prescimone, P. A. Wood, S. Parsons, S. P. Perlepes, G. Christou and E. K. Brechin, *J. Am. Chem. Soc.*, 2007, **129**, 6547-6561.

13 S. C. Xiang, S. M. Hu, T. L. Sheng, J. S. Chen and X. T. Wu, *Chem. Eur. J.*, 2009, **15**, 12496-12502.

14 G. Abbas, Y. H. Lan, V. Mereacre, W. Wernsdorfer, R. Clérac, G. Buth, M. T. Sougrati, F. Grandjean, G. J. Long, C. E. Anson and A. K. Powell, *Inorg. Chem.*, 2009, **48**, 9345-9355.

15 (*a*) S. X She, M. J. Zaworotko, W. Liu, Z. X. Zhang and Y. H. Li, *CrystEngComm*, 2013, **15**, 5003-5006; (*b*) S. X. She, Y. M. Chen, M. J. Zaworotko, W. Liu, Y. Y. Cao, J. Wu and Y. H. Li, *Dalton Trans.*, 2013, **42**, 10433-10438.

16 (*a*) F. Pointillart, K. Bernot, R. Sessoli and D. Gatteschi, *Chem. Eur. J.*, 2007, **13**, 1602-1609; (*b*) T. Yamaguchi, Y. Sunatsuki, H. Ishida, M. Kojima, H. Akashi, N. Re, N. Matsumoto, A. Pochaba and J. Mrozinski, *Inorg. Chem.*, 2008, **47**, 5736-5745; (*c*) T. Shiga, N. Ito, A. Hidaka, H. Ohkawa, S. Kitagawa and M. Ohba, *Inorg. Chem.*, 2007, **46**, 3492-3501; (*d*) J. P. Sutter, S. Dhers, R. Rajamani, S. Ramasesha, J. P. Costes, C. Duhayon and L. Vendier, *Inorg. Chem.*, 2009, **48**, 5820-5828; (*e*) J. -P. Costes, T. Yamaguchi, M. Kojima and L. Vendier, *Inorg. Chem.*, 2009, **48**, 5555-5561.

17 G. M. Sheldrick, *Acta Cryst.*, 2008, **A64**, 112-122.

18 (*a*) K. C. Mondal, B. Gole, Y. Song, S. R. Batten, D. R. Turner, and P. S. J. Mukherjee, *Chem. Sci.*, 2011, **123**, 807-818; (*b*) J. W. Zhao, J. Luo, L. J. Chen, J. Yuan, H. Y. Li, P. T. Ma, J. P. Wang and J. Y. Niu, *CrystEngComm*, 2012, **14**, 7981-7993; (*c*) J. W. Zhao, Y. Z. Li, F. Ji, J. Yuan, L. J. Chen and G. Y. Yang, *Dalton Trans*., 2014, **43**, 5694-5706.

19 G. F. Xu, Q. L. Wang, P. Gamez, Y. Ma, R. Clerac, J. Tang, S. P. Yan, P. Cheng and D. Z. Liao, *Chem. Commun.*, 2010, **46**, 1506-1508.

20 S. J. Liu, J. P. Zhao, W. C. Song, S. D. Han, Z. Y. Liu and X. H. Bu, *Inorg. Chem.*, 2013, **52**, 2103-2109.

21 X. M. Zhang, K. Wang, Y. Q. Wang and E. Q. Gao, *Dalton Trans.*, 2011, **40**, 12742-12749.

View Article Online
DOI: 10.1039/C6DT00951D

Two 3d-4f double helical chains including $[Dy_2M_2]_n$ (M = Ni^{II} and Co^{II}) cores exhibiting slow magnetic relaxation

Shixiong She, Yahong Li[*] and Wu Li

Two new heterometallic complexes with one-dimensional ladder-like double-helical chain structures were prepared.

They both exhibit interesting magnetic properties.